International Journal of Energy Systems and Mechanical Engineering
Volume1, Issue 1 2025

Energy and Exergy Investigation of a Solar Air Heater for Different Absorber Plate Configurations

Zhao, Xiangfeng, College of Locomotive and Rolling Stock Engineering, Nanjing Vocational Institute of Railway Technology, Nanjing, Jiangsu, China

Research Article

Date of Submission: 8-01-2025 Date of Acceptance: 12-02-2025 Date of Publication: 13-03-2025

ABSTRACT – This study examined the effects of various absorber plate designs, such as one line finned flat absorber and two lines finned absorber plate, on the thermal performance of a flat plate double passing solar air heater. In order to increase thermal efficiency, L-shaped fins are soldered onto the absorber plate to roughen it and create vortices that facilitate heat transmission between the absorber plate and the working fluid (air). The meteorological conditions of Baghdad city (longitude 33.3 N and latitude 44.44 E) were used for the outdoor experimental test between February and May. According to the findings, the air temperature for a single line of fins is 48 °C, 47.5 °C, and 58.5 °C at an air velocity of 1.7 m/s; for two lines of fins, it is 52 °C, 57.5 °C, and 66 °C at an air velocity of 0.9 m/s. At an air velocity of 0.9 m/s, the efficiency increases by 28% for one line of fins and 66% for two lines of fins; at an air velocity of 1.7 m/s, the efficiency increases by 27% and 51%, respectively. When the velocity rises from 0.9 m/s to 1.9 m/s, the average exergy destruction rate increases by 37.6%, 60.6%, and 68.66% for the absorber plate, working fluid, and glass cover, respectively. When the velocity increased from 0.9 m/s to 1.9 m/s, the exergy efficiency rose by 24.1%.

KEYWORDS

Double-pass solar air heater; Thermal performance;Flat solar air heater; Thermal efficiency; Finned surface

INTRODUCTION

Due to the growing world population and the substantial rise in energy use in contemporary life and business, energy demand has skyrocketed over the last three decades. It is common knowledge that increased use of conventional energy sources, such as fossil fuels, will have a significant impact on pollution levels, global warming, and energy costs. Solar energy, a sustainable renewable energy source, has emerged as a key area of study to mitigate these consequences. It is distinguished by being a significant source of sustainable, cost-free, and green energy [1-2]. According to recent studies [3-6], system development to enhance thermal energy conversion performance is a promising area of study with several useful applications around the globe. By adding fins, baffles, and turbulators—which also produce turbulence—to increase the surface area of heat exchange, industrial product development procedures may also enhance energy efficiency. Thermal fluids with improved thermophysical characteristics of nanofluids are another way to boost efficiency. Nanofluids, which were thought to have a high capacity because of their high thermal conductivity, replaced the conventional fluids used in heat transfer applications [7]. They are frequently used in heat transfer applications to boost the energy efficiency of various devices [8–10]. Solar radiation may be converted into thermal energy for heating and cooling purposes using a variety of thermal solar collectors. Solar air heaters (SAH) are solar panels that transform solar radiation into thermal energy that may be used to dry crops or warm dwellings. SAHs stand out for their inexpensive production costs, ease of use, and lack of environmental and health risks. There are many different SAH designs that are categorized according on the airflow inside them, both single-pass and double-pass.

The evolution of heat systems' thermal performance employing fins, baffles, and turbulators has been studied by several researchers. For surface-modified solar air heaters, Kumar [11] investigated the friction characteristics and heat transmission under laminar flow conditions. The inner surface of a rectangular duct and a roughened V-corrugated absorber plate were used. The redesigned absorber plate shows a greater heat transfer rate with a larger friction loss, according to the data. Jia [12] examined how a modified solar air heater with a folding spoiler affected the absorber plate's irradiance

and air volume flow rate. It has been found that the modified solar air heater is more efficient than the traditional one. Abdullah [13] experimentally investigated the impact of aluminum can tabulators and external reflectors on a single-pass SAH's performance. Three different absorber plate designs were tested: staggered-cans roughened plate, cans-line roughened plate, and smooth plate. At the intake, air guidance vanes were installed. It was discovered that the efficiency improvement was 73%. Dezan [14] looked at how winglet pairs affected a SAH's performance. The chord length, angle of attack, and winglet height were the parameters that were investigated. The friction factor was shown to be more responsive to the examined factors than the Nusselt number. Jouybari [15] used a thin porous media layer to examine the impact of coating on a SAH's absorber plate. It was discovered that the thin porous layer increased friction loss by 200% and enhanced thermal performance by 500%. The efficacy of a tubular solar heater (TSAH) with an absorber shaped like a sheet of neighboring tubes was investigated experimentally by Hassan [16]. In comparison to traditional SAH, the improved tubular solar heater's efficiency and air temperature were found to be 132% and 13 °C higher, respectively. A SAH roughened with S-shaped ribs with gaps was created by Wang [17]. The roughened SAH increased heat efficiency by 13% to 48%, according to the studies. The thermal performance of arc-shaped roughened solar air heaters with apex up and apex down airflow was examined experimentally by Ghritlahre [18]. The airflow rates used in the tests ranged from 0.007 to 0.022 kg/s. The findings demonstrated that efficiency rose as airflow rates increased, reaching 73.2% at the apex upstream flow and 69.4% at the apex downstream flow at a mass flow rate of 0.022 kg/s. Two triple-pass SAHs' performances were compared by Yassien [19]. One features a network of tubes under the absorber plate, while the other has a double glass cover. According to the findings, the first model's efficiency is greater than the second's, at 80.2% and 73.4%, respectively. Baissi [20] investigated how a SAH's performance was affected by the perforation of delta-shaped baffles. The findings demonstrated that the use of baffles increased heat transmission. For perforated and non-perforated baffles, the highest thermal enhancement factor (TEF) rate was 2.26 and 2.21, respectively. The impact of roughened absorber plates with rectangular, triangular, and elliptical fins on the performance of a SAH for various inclination angles was examined statistically by Ranjbar [21]. The efficiency of SAH with rectangular fins was found to be 12.5% and 5.5% greater, respectively, than that with elliptical and triangular fins. Additionally, it was said that the ideal angle was between 50° and 70°. Saravanan and colleagues [22] looked at

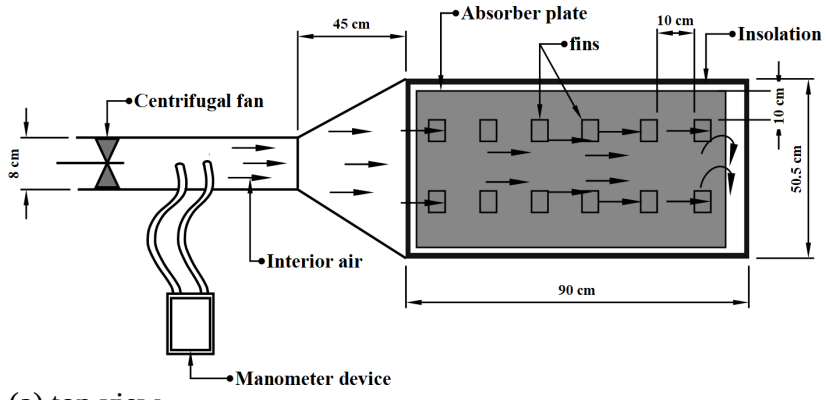
The effectiveness of a solar air heater with perforated and non-perforated C-shaped fins was tested. It was discovered that the heat transfer rate is increased by 2.67 when perforated fins are used.
Numerous researches have looked at the impact of utilizing nanofluids in SAH. The impact of base fluid volume on the thermal performance and entropy production of parabolic trough collectors (PTCs) was examined by Olia [23]. It was shown that although nanofluids may lower the system's entropy production and improve heat transfer and thermal efficiency, they also increase the pressure drop. The second law of thermodynamics was used to study the thermodynamics of the turbulent flow of the nanofluid in a solar heating channel with the roughness of the rib on the absorber plate [24]. The effects of a variety of variables were examined, including friction, the concentration of nanofluid on thermal reflections, Reynolds number, angle, height, and degree of rib employed on the absorbent plate. According to the findings, the creation of thermal entropy was reduced by around 11.1% when nanofluids with a concentration of 0.04 were used. Additionally, for Re = 3200, raising the rib height in the range of 0.025-0.033 reduced the formation of thermal entropy by around 21.05%. A study of pulsed flow in a three-dimensional channel was published in [25], where the turbulent and laminar flows inside the channel were examined. The impact of several transverse channel shapes, including triangle, hexagon, and circular, with pulsed flow was also examined. Alumina nanofluids (Al2O3) were used as a working fluid in different ratios (0 percent [clean water], 3 percent, and 5 percent) to show how they affected temperature, velocity, and pressure. The findings shown that as the proportion of liquid volume increases, Al2O3 can provide energy at a steady temperature. According to the literature study, there are several research projects aimed at enhancing solar air heater performance. The effectiveness of solar air heaters may still be improved for the local weather conditions in

Baghdad, Iraq, despite these research efforts and a huge number of published articles. This research's broad variety of applications and contribution to mitigating the greenhouse impact make it significant. Thus, the purpose of this article is to examine how the L-shaped fins and intake air velocity affect the solar air heater's efficiency. In order to accomplish this goal, a series of tests were carried out under clear sky circumstances over many days in 2019, from February to May. Ten hours a day, the data were gathered every hour. Three measured air velocities were 1.9 m/s, 1.7 m/s, and 0.9 m/s.

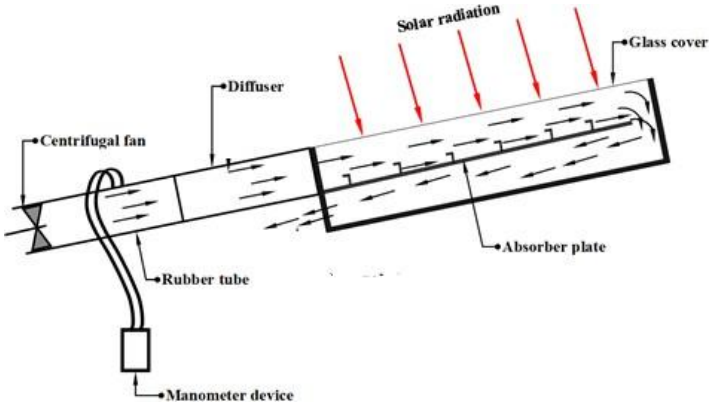
EXPERIMENTAL SETUP

The current study's experimental setup was created, constructed, and set up on the roof of Al-Esraa University College in Baghdad, Iraq (33.3 N longitude and 44.44 E latitude). As shown in Figures 1 and 2, the experimental setup is a double-pass solar air heater. The solar air heater is composed of a rectangular box constructed from two-millimeter-thick PVC sheets. The solar heater's inside measurements are 90 x 50.5 x 16 cm. To reduce heat loss to the environment, the solar heater's inside sides are insulated with two layers of cork and ArmaFlex that are 2 cm and 1 cm thick, respectively. The glass cover of the solar heater measures 69 by 49 cm and is 3 mm thick. A 70 x 50 cm copper flat absorber plate serves as the partition wall between the solar heater's top and bottom channels. To improve the plate's ability to absorb solar energy, it is coated black. Copper fins in the form of a L are soldered to the absorber plate's top face.

For the first configuration, six fins are soldered in a line, and for the second configuration, six more fins are soldered in a second line parallel to the first, making a total of twelve fins. An iron plate covers the bottom of the solar heater, which is in the lower pass. This plate absorbs heat from the copper absorber plate's lower face and retransfers it to the air traveling through the lower pass before it exits the solar heater. A unique 45-cm-long metallic diffuser allows air to enter the heater. The diffuser has a rectangular output of 50.5 x 8 cm and a circular intake with a diameter of 7.5 cm. At the conclusion of the lower pass, a rectangular opening measuring 50.5 by 8 cm allows the air to depart the solar heater. A centrifugal blower that is attached to the diffuser via a rubber hose provides the air to the solar heater. A coating of thermal wool is used to insulate the hose. An adjustable gate located at the blower's suction port regulates the air's velocity. The experimental setup is shown in Figure 3. Six thermocouples of type (K) linked to a data logger of type BTM-4208SD are used to measure the temperatures. The temperature of the absorber plate is measured using three thermocouples. The temperature of the air at the solar heater's entrance and exit is measured by two thermocouples. The insulation's internal temperature is measured using a single thermocouple. An anemometer is used to measure wind speed. The Iraqi Ministry of Science and Technology is the source of the sun radiation statistics for Baghdad.



(a) top view



(b) side view

Figure 1. Experimental solar air heater system

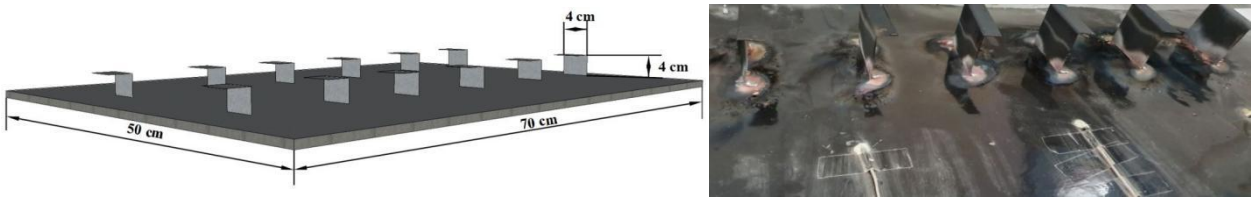


Figure 2. Absorber plate with fins

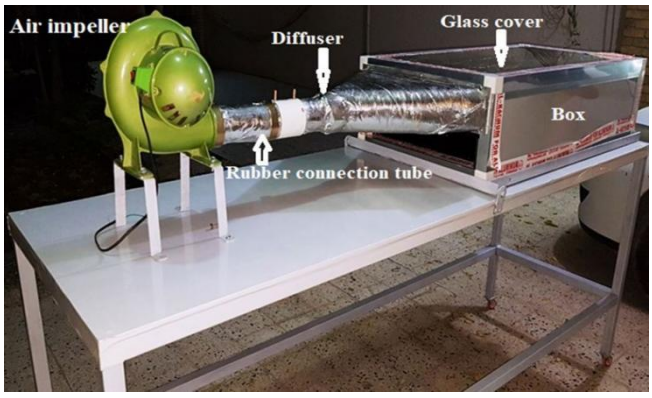


Figure 3. Test rig

THERMAL PERFORMANCE OF SOLAR AIR HEATER

The air velocity is varied for all experiments and temperatures are measured at the inlet and outlet of the flowing air and at different locations of the absorber plate. The heat balance of the solar air heater requires the calculations of heat input from solar radiation and the heat losses from the walls. Figure 4 shows the thermal resistance of the SAH used to compute the overall heat transfer coefficient. The heat transfer coefficient of the insulated side walls (edges) of the solar air heater (U_E) is in Eq. (1) [26]:

$$U_E = \frac{K_{insu} A_E}{L} \quad (1)$$

The heat transfer coefficient of the insulated bottom side wall of the solar air heater (U_B) [26] is:

$$U_B = \frac{K_{insu} A_B}{L} \quad (2)$$

The heat transfer coefficient of the top side of the solar air heater (U_F) [26] is in Eq. (3):

$$U_F = \left[\frac{1}{h_{r,gg-sky} + h_{c,gg-amb.}} + \frac{1}{h_{r,p-gg} + h_{c,p-gg}} \right]^{-1} \quad (3)$$

The radiation heat transfer coefficient ($hr,p-gg$) between the absorber plate and the glass cover can be calculated by Eq. (4) [27]:

$$\sigma(T_p + T_{gg})(T^2 + T^2) \quad 4\sigma(T^2) \quad h \qquad = \qquad p \qquad (4)$$

$$gg \approx \qquad p$$

$$r,p^{-}gg \quad \frac{1}{\varepsilon\varepsilon_p + \varepsilon\varepsilon_{gg} - 1} \quad \frac{1}{\varepsilon\varepsilon_p + \varepsilon\varepsilon_{gg} - 1} \quad \frac{1}{}$$

The convection heat transfer coefficient from the absorber plate to glass cover ($hc,p-gg$) [26] is calculated by:

$$h_{c,p-gg} = \frac{Nu.\, k_{air}}{D} \qquad (5)$$

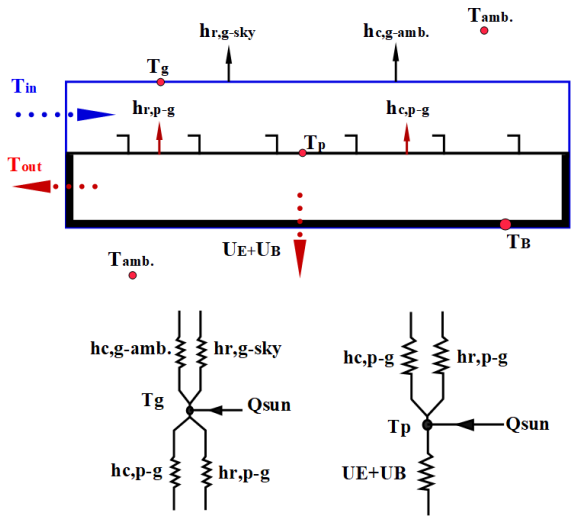


Figure 4. Heat transfer network and schematic of solar air heater thermal losses Nusselt number of the solar air heater is calculated by Eq. (6) [26]:

$$Nu = 0.0158(Re)^{0.8} \qquad (6)$$

The convective heat transfer coefficient of the wind at the outer surface of the glass cover ($hc,gg-amb.$) as presented in Eq. (7) and (8) [26]:

$$h_{c,gg-amb.} = 2.8 + 3\,V_{ww} \qquad (7)$$

$$h_{c,gg-amb.} = 5.7 + 3.8\ V_w \qquad (8)$$

The radiative heat transfer coefficient between the outer surface of the glass cover and the sky ($hr,gg-sky$), it is given as Eq. (9) [28]:

$$4 \qquad 4 \qquad (9)$$

$$h_{r,gg-sky} = \varepsilon\varepsilon_{gg}\sigma\ \text{[illegible]}(T_{gg} + 273)\ -(T_{sky} + 273)\ \text{[illegible]}/(T_{gg} - T_{sky})$$

Different models are available for the effective sky temperature. According to Duffie and Beckman [24], the sky temperature is determined as:

$$T = T \quad \text{0.711} + 0.0056T + 0.000073T^2 + 0.013\cos(15t) \quad (10)$$

1/4

$sky \quad amb. \quad dp \quad dp$

where T_{sky} and $T_{amb.}$ (ambient temperature) are in (K), t is an hour from midnight. Alfegi et al. [29] gave the following equations for sky temperature:

$$T_{sky} = 0.0552(T_{amb.})^{1.5} \quad (11)$$

Or,

$$T_{sky} = T_{amb.} - 6 \quad (12)$$

Equations (11) and (12) are only applicable in humid climates. When the dew point temperature or relative humidity is available, Eq. (10) is utilized; otherwise, Eq. (11) is utilized. The total amount of heat lost from the SAH (U_T) [24] is:

$$U_T = U_F + U_E + U_B \quad (13)$$

Heat loss from The SAH (QQ_{losses}) is calculated as follows [26]:

$$QQ_{losses} = U_T A_h (T_p - T_{in}) \quad (14)$$

where A_h is the solar air heater upper surface area (m^2). The heat gain of the flowing air can be determined as follows [26]:

$$QQ_{ggain} = \dot{m} cp (T_{out} - T_{in}) \quad (15)$$

$$\dot{m} = \rho v A \quad (16)$$

The thermal performance of the solar air heater is related to the heat transfer from the absorber plate and the heat collection efficiency. The thermal efficiency of the solar air heater can be calculated as follows:

$$\eta = \frac{\text{Thermal power transferred to fluid}}{\text{Thermal power received by absorber}} \quad (17)$$

$$\eta = \frac{QQ_{ggain}}{I A_P} = \frac{\dot{m} cp (T_{out} - T_{in})}{I A_P} \quad (18)$$

EXERGY ANALYSIS OF THE SOLAR AIR HEATER

Exergy analysis applied to a solar collector aid in the creation of an optimal design and provides guidance on how to reduce exergy losses. The Exergy principle is one of two approaches to the second law analysis, with the other being entropy creation from irreversibilities. Both approaches provide essentially the same outcomes. Maximizing exergy efficiency can help to reduce the amount of exergy lost during thermodynamic processes. In an environment with a temperature of T_a, the optimum work may be done by transferring energy from a heat source with a temperature of T. Exergy with the amount of Ex_{heat} is always companion with heat transfer QQ at a location at a thermodynamic temperature
T [30]. The applied assumptions in this model are:
Steady flow operation.
Steady-state heat transfer.
The fluid is incompressible.
Negligible the effects of kinetic and potential energy.
There are no nuclear or chemical reactions in the system.

$$Ex_{heat} = QQ \left(1 - \frac{T_{amb.}}{T}\right) \quad (19)$$

where $(1 - \frac{T_{amb.}}{T})$ is the Carnot coefficient factor. In general, Eq. (20) is implemented to derive the exergy balance

of each element of the SAH [30,31]:

$$Ex_{in} - Ex_{out} - Ex_{accu} - Ex_{dest} = Ex_{sys} \quad (20)$$

Figure 5 shows the exergy exchange between the different components of the SAH [32, 33].

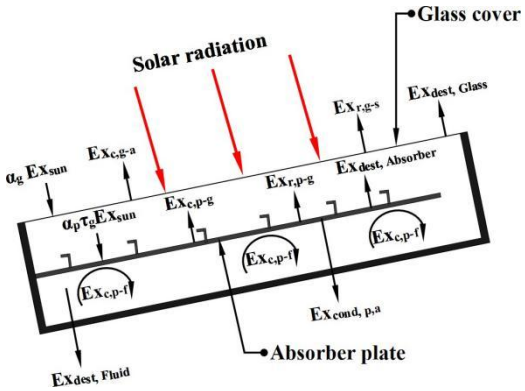


Figure 5. Exergetic flow diagram in solar air heater

Glass Cover Exergy

The exergetic balance of the glass cover is:

$$Ex_{\text{dest , Glass}} = \alpha_{gg} Ex_{\text{sun}} + Ex_{r,p-gg} + Ex_{c,p-gg} - Ex_{c,gg-a} - Ex_{r,gg-s} \quad (21)$$

The sum of the exergy absorbed by the glass cover from the sun ($\alpha_g Ex_{sun}$) and the radiative ($Ex_{r,p-gg}$) and convective exergy ($Ex_{c,p-gg}$) transferred from the absorber plate to the glass cover represents the exergy gained by the glass cover. Part of the absorbed exergy is lost to the environment by convective ($Ex_{c,gg-a}$) and radiative ($Ex_{r,gg-s}$) exergy transfer, while the remainder is destroyed ($Ex_{\text{dest , Glass}}$). Ex_{sun} is the result of the Petela expression [32-34] and the incident solar radiation G.

$$Ex_{sun} = GS_{gg}\left[1 + \frac{1}{3}\left(\frac{T_a}{T_s}\right) - \frac{4}{3}\left(\frac{T_a}{T_s}\right)\right] \quad (22)$$

where T_S is the sun temperature and is ssumed to be 6000 K. ($Ex_{r,p-gg}$) is the radiative exergy transferred from the abrorber plate to the glass cover and given by:

$$Ex_{r,p-gg} = h_{r,p-gg} S_{gg} (T_p - T_{gg}) \left[1 + \left(\frac{1}{3}\right)\left(\frac{T_p}{T_{gg}}\right) - \left(\frac{4}{3}\right)\right] \quad (23)$$

($Ex_{c,p-gg}$) is the convective exergy transferred from the absorber plate to the glass cover and given by:

$$Ex_{c,p-gg} = h_{c,p-gg} S_{gg} (T_p - T_{gg}) \left(1 - \frac{T_a}{T_p}\right) \quad (24)$$

($Ex_{c,p-gg}$) is the convective exergy lost from the glass cover to the environment and given by:

$$Ex_{c,gg-a} = h_{c,gg-a} S_{gg} (T_{gg} - T_a)\left(1 - \frac{T_a}{T_{gg}}\right) \quad (25)$$

($Ex_{r,gg-s}$) is the radiative exergy lost from the glass cover to the sky and given by:

$$Ex_{r,gg-s} = h_{r,gg-s} S_{gg} (T_{gg} - T_{sky}) \left[1 + \left(\frac{1}{3}\right)\left(\frac{T_{gg}}{T_{gg}}\right) - \left(\frac{1}{3}\right)\right] \quad (26)$$

Absorber Plate Exergy

The exergy balance of the absorber plate is:

$$Ex_{dest,\ Absorber} = \alpha_p \tau_{gg} Ex_{sun} - Ex_{r,p-gg} - Ex_{c,p-gg} - Ex_{cond,p-a} - Ex_{c,p-f} \quad (27)$$

where $Ex_{cond,p-a}$ is the conductive exergy transferred from the absorber plate to the surroundings and given as:

$$Ex_{cond,p-a} = \frac{k_i}{\delta\delta_i} S_p(T_p - T_a)\left(1 - \frac{T_a}{T_p}\right) \quad (28)$$

and $Ex_{c,p-f}$ is the convective exergy transferred from the absorber plate to the working fluid and expressed as:

$$Ex_{c,p-f} = h_{c,p-f} S_{ech} (T_p - T_f)\left(1 - \frac{T_a}{T_p}\right) \quad (29)$$

Working Fluid Exergy

The exergy balance of the working fluid is written as [35,36]:

$$Ex_{d,f} = h_{c,p-f} S_{ech}(T_p - T_f)\left(1 - \frac{T_a}{T_p}\right) - \dot{m}_f C_{p,f} \left[(T_{out} - T_{in}) - T_a \ln\left(\frac{T_{out}}{T_{in}}\right)\right] \quad (30)$$

Solar Collector Exergy Efficiency

The exergy efficiency (η_{ex}) of the flat-plate solar collector is defined as the ratio of exergy gained by the working fluid to the exergy input to the SAH [37].

$$\eta_{ex} = \frac{\dot{m}_f C_{p-f} \left[(T_{out} - T_{in}) - T_a \ln\left(\frac{T_{out}}{T_{in}}\right)\right]}{GS_{col}\left[1 + \frac{1}{3}\left(\frac{T_a}{T_s}\right) - \frac{4}{3}\left(\frac{T_a}{T_s}\right)\right]} \quad (31)$$

EXPERIMENTAL ERROR ANALYSIS

The approach given by Holman [38] is adopted, to calculate the error in the acquired results. The proportion error of the solar air heater system efficiency is calculated as:

$$WW_S = \left[\left(\frac{\partial S}{\partial x_1} WW_1\right)^2 + \left(\frac{\partial S}{\partial x_2} WW_2\right)^2 + \cdots + \left(\frac{\partial S}{\partial x_n} WW_n\right)^2\right]^{1/2} \quad (32)$$

From the equation of thermal efficiency (η), the uncertainty of efficiency can be derived (following Eq. (19)) as:

$$WW_\eta = \left[\left(\frac{\partial \eta}{\partial \Delta T} WW_{\Delta T}\right)^2 + \left(\frac{\partial \eta}{\partial m} WW_m\right)^2 + \left(\frac{\partial \eta}{\partial A} WW_A\right)^2 + \left(\right.\right. \quad (33)$$

$$\frac{\partial \Delta T}{\partial m} \quad \frac{WW_l)^2 \blacksquare}{\partial A_p} \quad {}^{p} \quad \frac{}{\partial I}$$

The uncertainties of measured and resulting data are shown in Table 1.

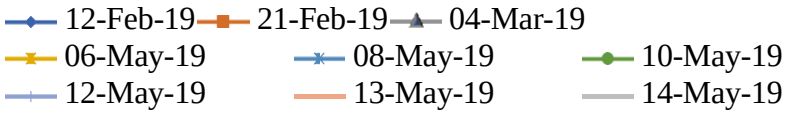
Table 1. Uncertainties of measured and resulted data

Parameter	Uncertainty
Air temperature difference	±2.3 (℃)
Mass flowrate ($\dot{m}_{air}$)	±0.03 (kg/s)
Solar radiation	±1.6 (W/m^2)
Heater area	±0.8 (m^2)
Thermal efficiency	±3.5 (%)

RESULTS AND DISCUSSION

The experimental measurements are conducted under clear sky circumstances from December 2, 2019, to May 14, 2019. Three air velocities—1.9 m/s, 1.7 m/s, and 0.9 m/s—are used to display the findings. To reduce the impact of clouds on direct solar radiation, the measurements are taken for ten hours every day under almost clear skies.

The distribution of solar radiation intensity with local time for each experiment day is shown in Figure 6. From the early hours of the day, the sun intensity progressively increases until it reaches its peak at midday, after which it gradually decreases. The sunlight intensity on May 12 is 409 W/m2 at 8:00, rises to 918 W/m2 at 12:00, and then decreases from the afternoon until dusk. The average daily values of solar intensity may be roughly regarded as steady since they vary between 440 W/m2 and 346 W/m2, according to the calculation of the average solar intensity for each experiment day.



1000

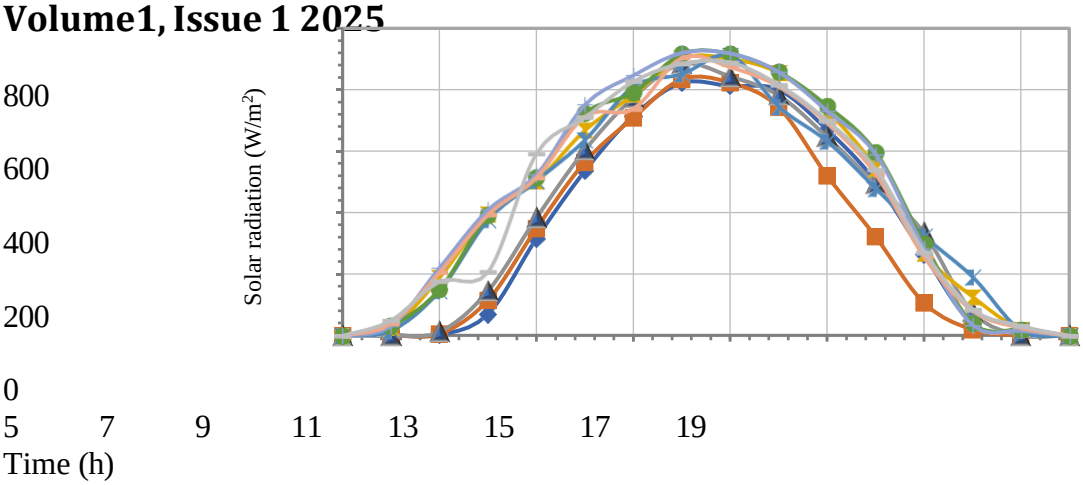
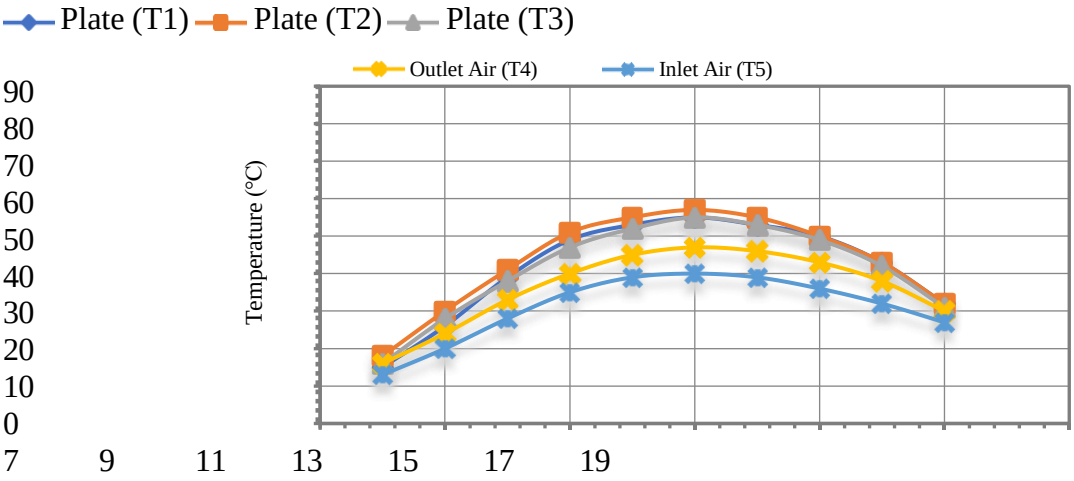
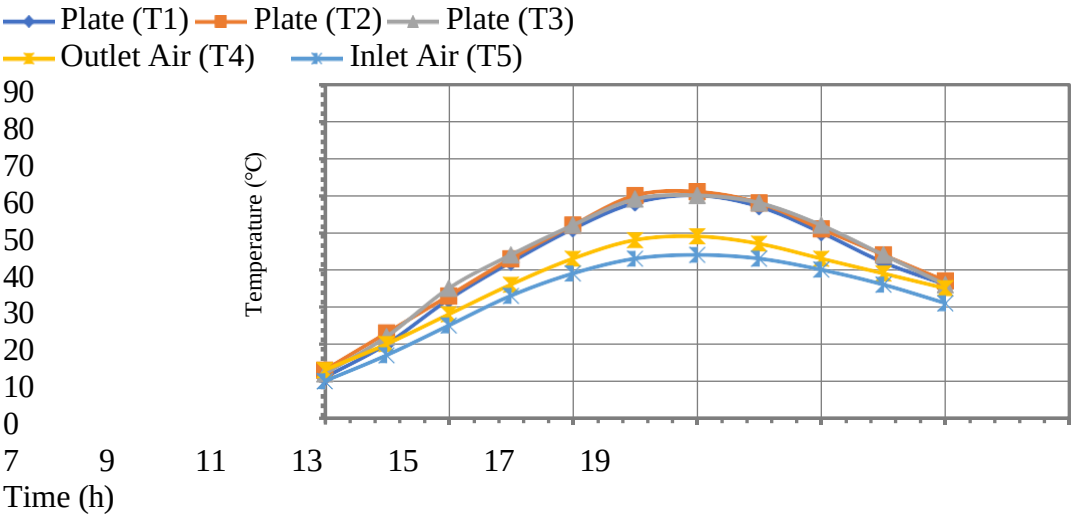


Figure 6. The hourly variation of solar irradiance

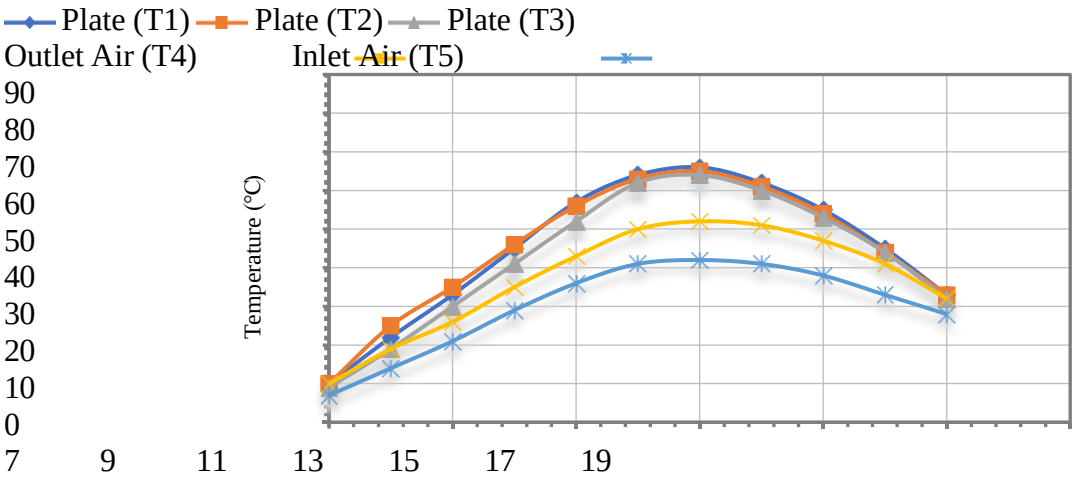
Figure 7(a) to 7(c) show the temperature profiles of the absorber plate and air versus time for the SAH with smooth absorber plate for the velocities 1.9 m/s, 1.7 m/s and 0.9 m/s, respectively. In general, the temperatures of plate, air inlet and air outlet were found to be rising exponentially from the early morning to reach the maximum values at noon and then fall gradually during the day with some fluctuations through some days. The maximum air temperatures at the exit are 48 ℃, 49 ℃ and 52 ℃ for velocities of 1.9 m/s, 1.7 m/s and 0.9 m/s, respectively. This means that the lower air velocity, the higher air temperature. This behavior can be rationalized as, at low velocity the air spends more time in contact in the upper and lower pass of the double-pass solar air heater.



at v=1.9 m/s (on 12-Feb-2019)



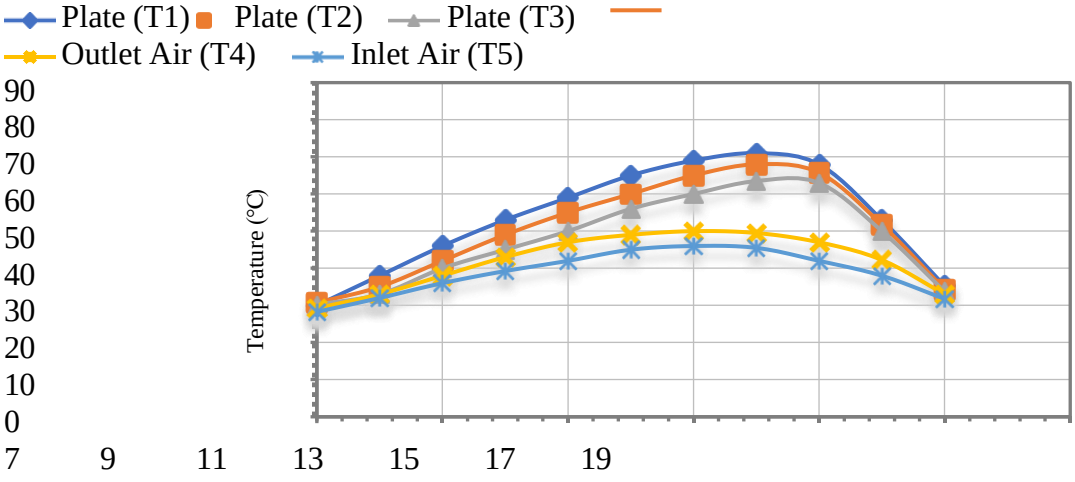
at v = 1.7 m/s (on 21-Feb-2019)



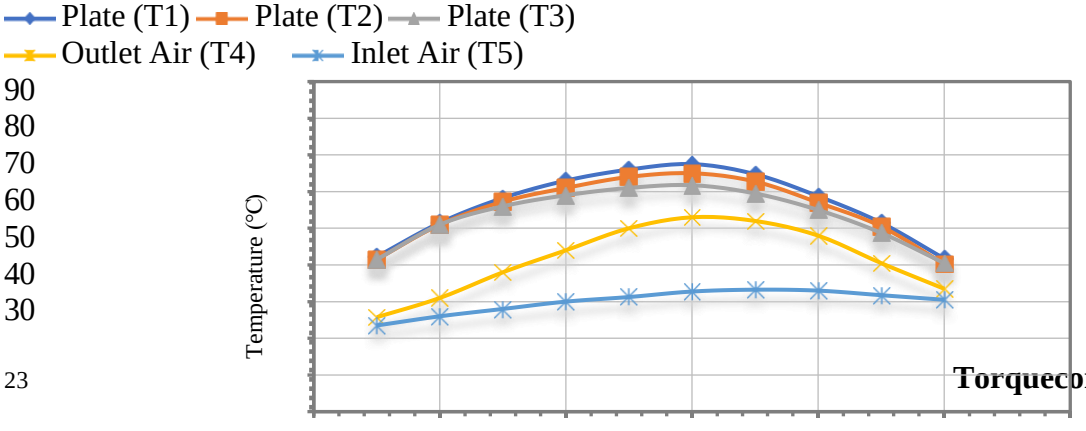
at v = 0.9 m/s (on 4-March-2019)

Figure 7. The hourly variation of temperatures inside the solar air heater without fins

Figures 8(a) to 8(c) show the temperature profiles of the absorber plate and air versus time for the SAH with one line of fins (6 fins) - absorber plate for the velocities of 1.9 m/s, 1.7 m/s and 0.9 m/s respectively. The effect of fins on the air temperature at the exit is clear as the air maximum temperature increased from 48 °C, 49 °C and 52 °C for a smooth plate to 50 °C, 52 °C and 57 °C of an online finned plate at velocities of 1.9 m/s, 1.7 m/s and 0.9 m/s, respectively. The increase is attributed to the increased surface area of the absorber plate and the generated turbulence. The comparison between the maximum air temperature for different days is justified because the range of the variation of average solar intensity is small.



at v=1.9 m/s (6-May-2019)



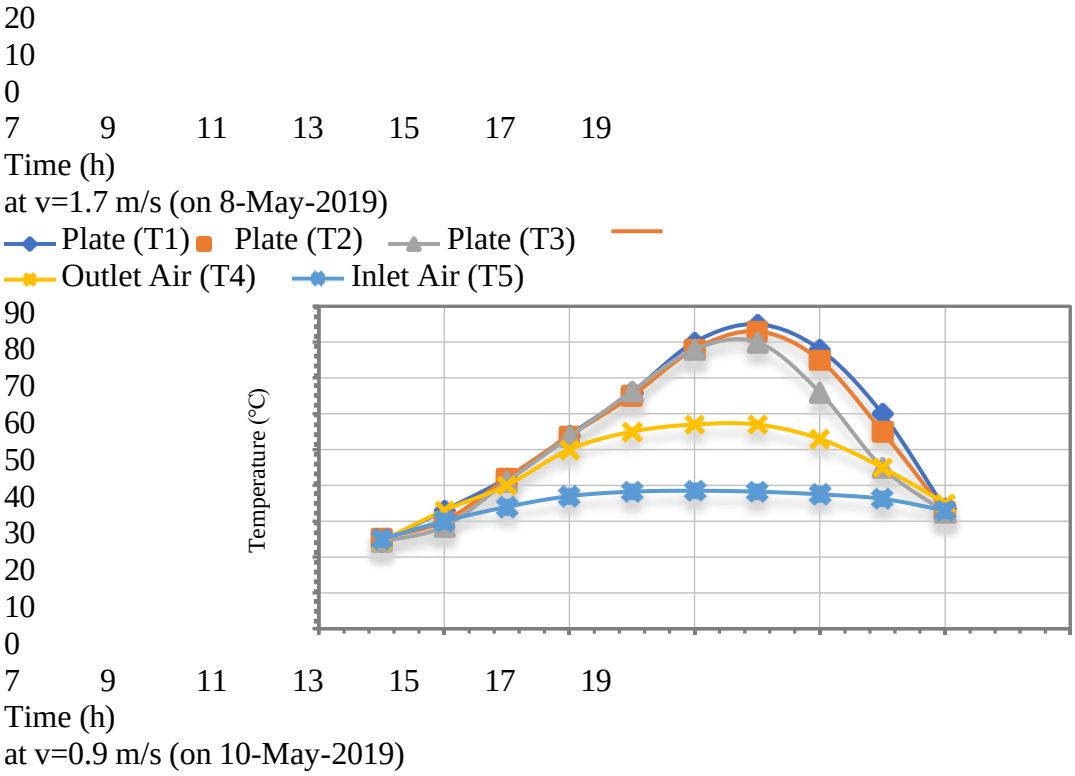
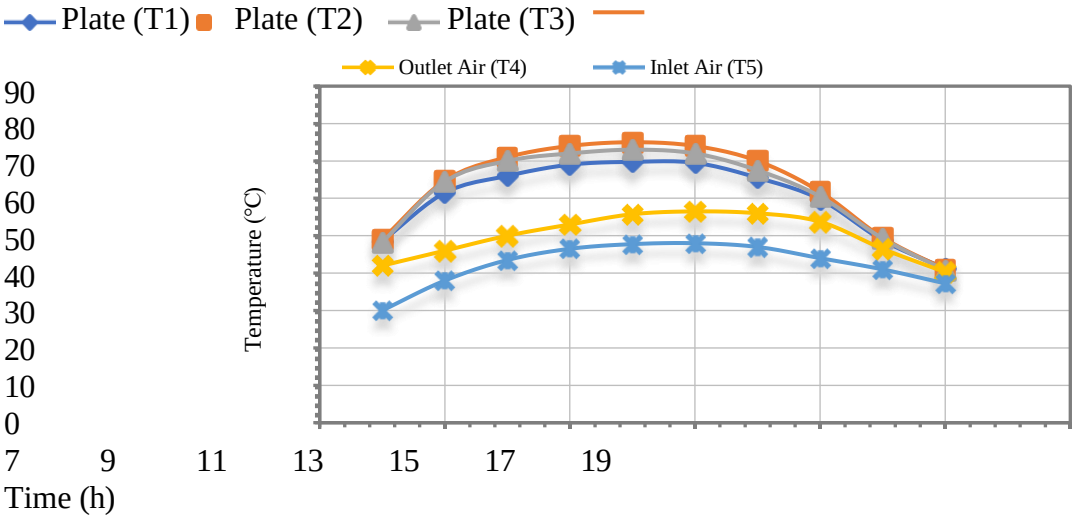
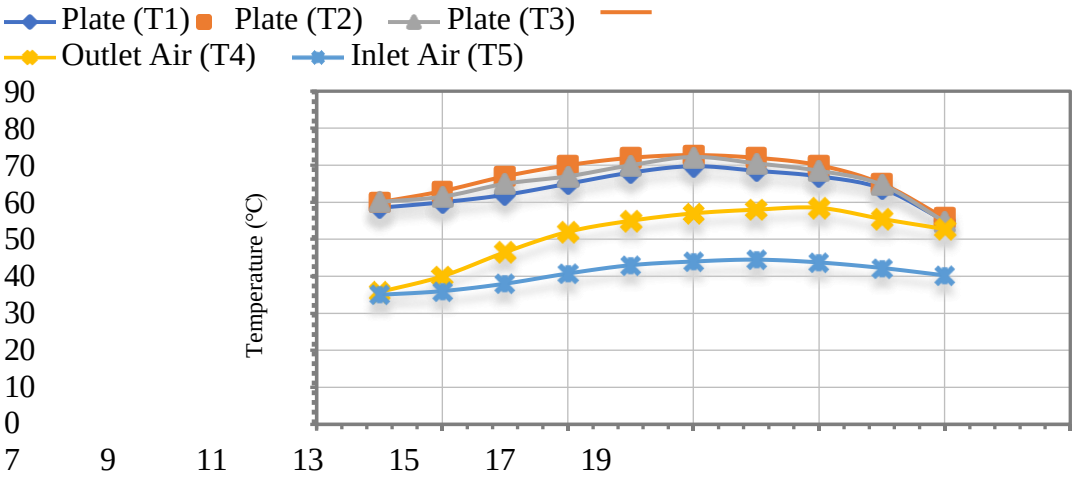


Figure 8. Hourly variation of temperatures inside the solar air heater in case of one line of fins

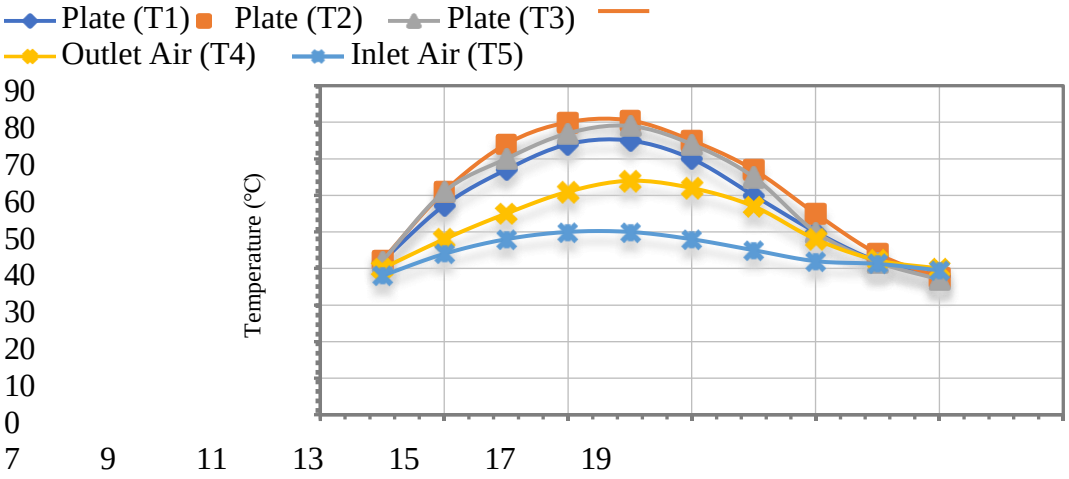
Figure 9(a), 9(b) and 9(c) show the temperature profiles of the absorber plate and air versus time for the SAH with two lines of fins (12 fins) - absorber plate for the velocities of 1.9 m/s, 1.7 m/s and 0.9 m/s. The effect of two lines of fins on the air temperature at the exit is more significant as the air maximum temperature increased from 50 °C, 52 °C and 57
°C for one line finned plate to 56.5 °C, 58.5 °C and 64 °C for two lines finned plate for velocities of 1.9 m/s, 1.7 m/s and
0.9 m/s respectively. This greater effect of the fins on the temperature of the air for two lines of fines is attributed to the larger surface area and the larger turbulence generation rate due to the greater fin number.



at v=1.9 m/s (on 12-May-2019)



at v=1.7 m/s (on 13-May-2019)



at v=0.9 m/s (on 14-May-2019)

Figure 9. Hourly variation of temperatures inside the solar air heater in case of two lines of fins

Efficiency Variation with Time of the Day

Figures 10(a) to 10(c) illustrate the efficiency variation of the double pass solar air heater with local time at different air velocities for smooth, one line of fins, and two lines of fines absorber plates. Because efficiency is a function of solar intensity, it rises early in the day, reaches its maximum levels about 13:00, and then progressively declines. The fins on the absorber plate have a significant impact on efficiency. When compared to the efficiency of the smooth plate, the average efficiency is increased by 28% and 66%, respectively, for one line and two lines of fins at a velocity of 1.9 m/s. When compared to the efficiency of the smooth plate, the average efficiency is increased by 27% and 51% for one line and two lines of fins, respectively, at a velocity of 1.7 m/s. When compared to the efficiency of the smooth plate, the average efficiency is increased by 21% and 50% for one line and two lines of fins, respectively, at a velocity of 0.9 m/s. These findings show that, under the present experimental circumstances, adding fins to the double-pass air solar heater increases the average efficiency by 21% to 66%.

Table 2 compares the efficiency of the current solar air heater with previously evaluated SAHs in the literature in order to confirm the findings. The effectiveness of the current work shows a strong correlation with those found in the literature.

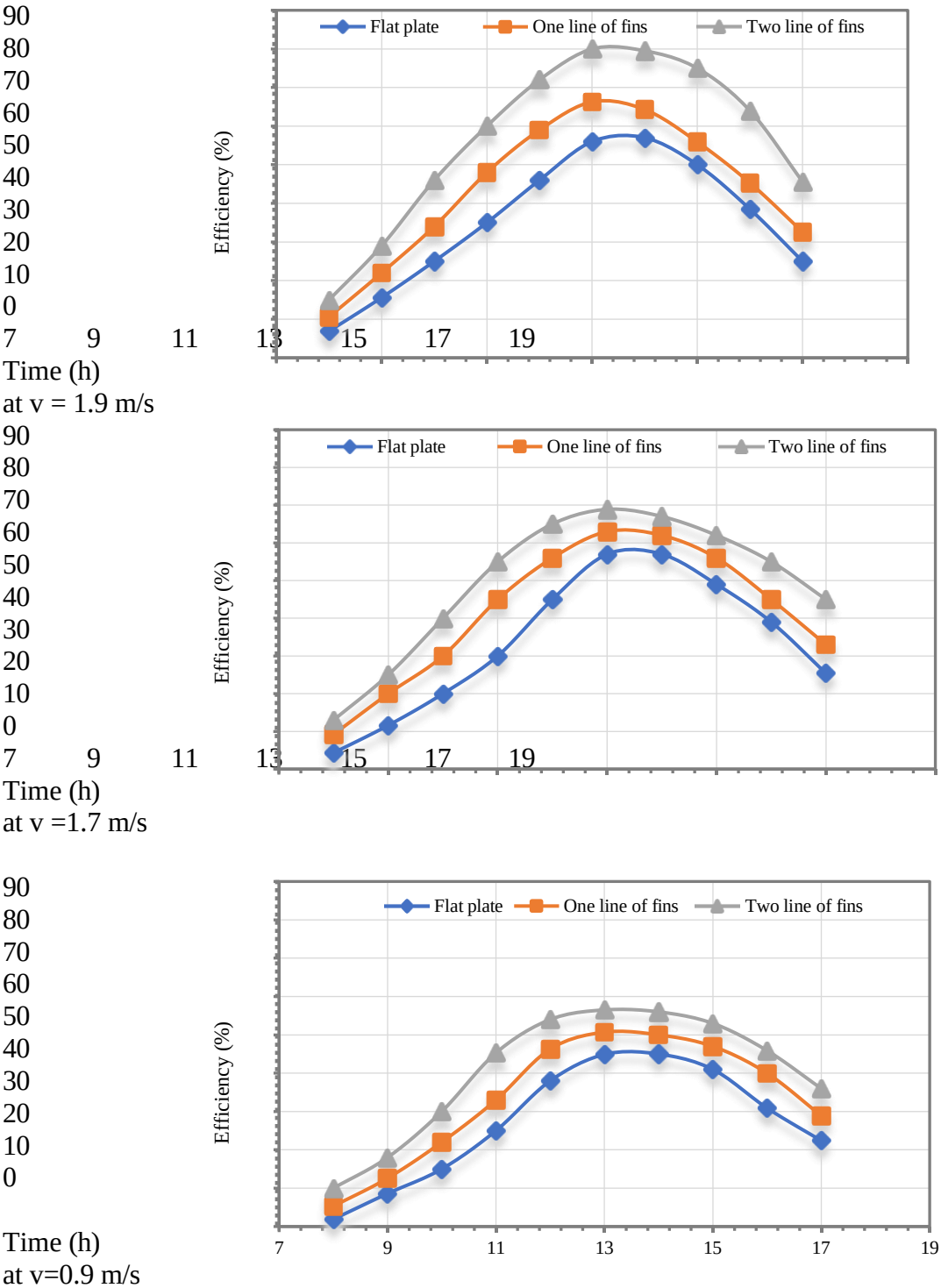
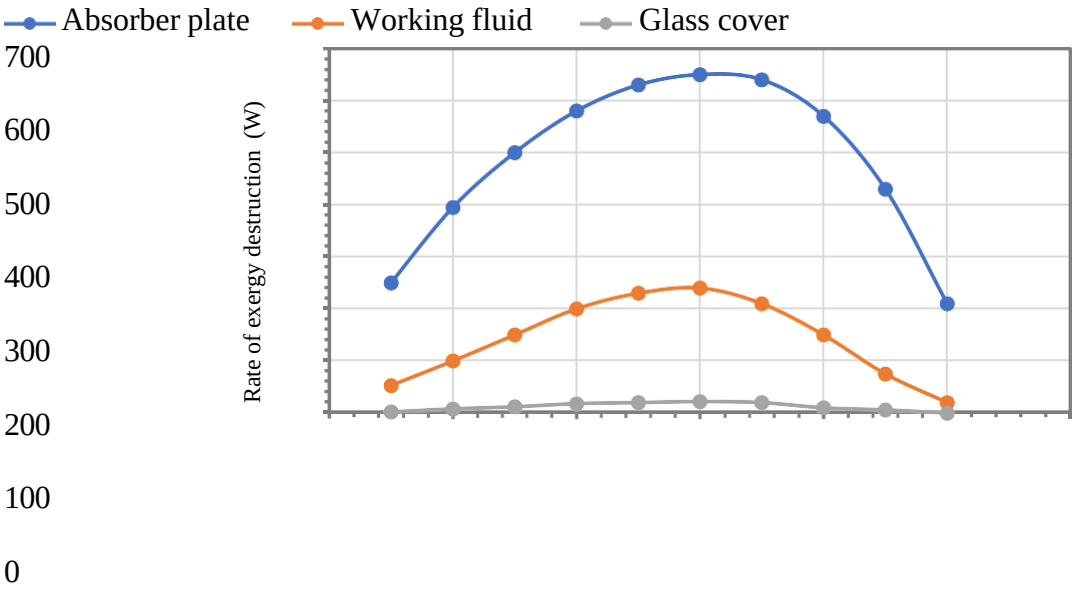


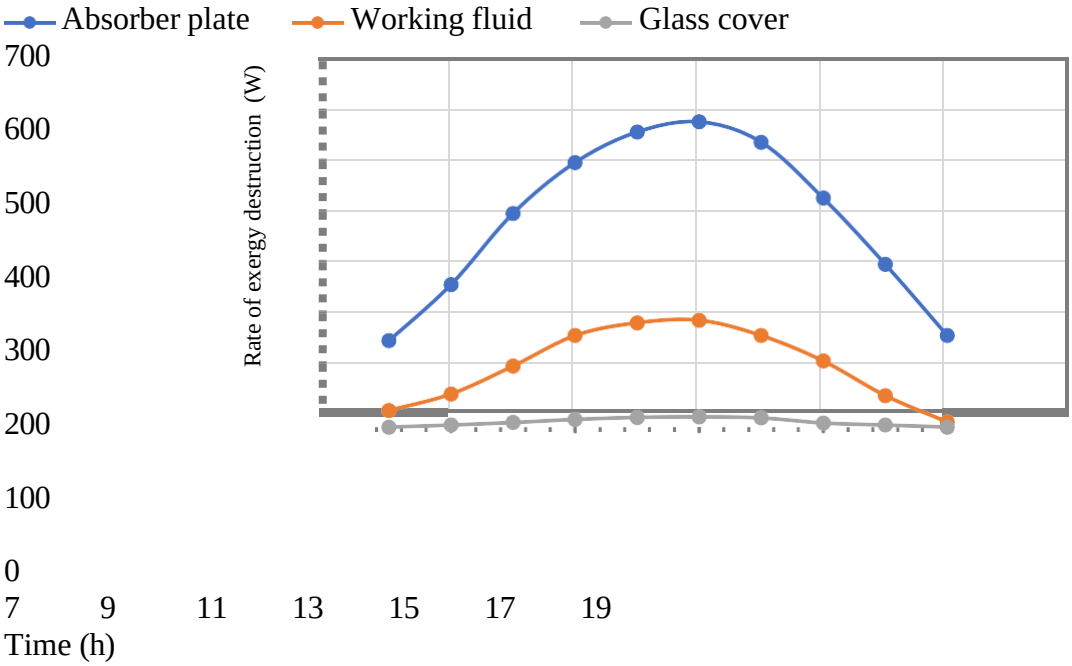
Figure 10. The hourly variation of thermal efficiency for solar air heater

Daily Variation in Components Exergy Destruction Rates

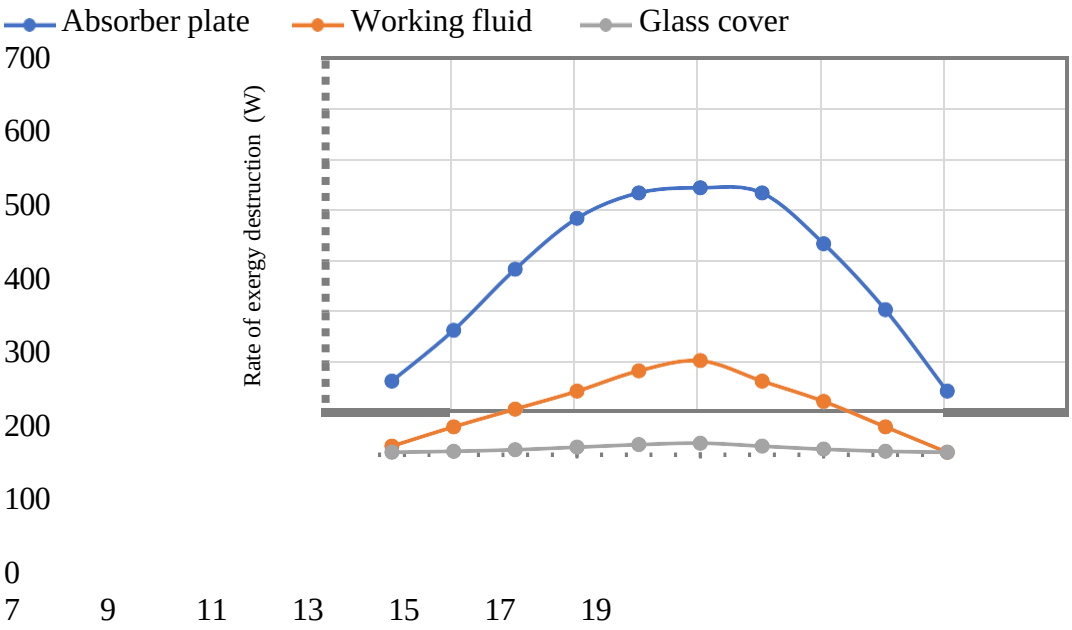
Figures 11(a) to 11(c) show the findings for different velocities (v = 1.9 m/s, 1.7 m/s, and 0.9 m/s) of the rate of exergy destruction for the solar air heater's components with two lines of fins: the absorber plate, glass cover, and working fluid. Exergy destruction rates are correlated with solar intensity, with the maximum solar intensity corresponding to the highest exergy destruction rate. Due to minute temperature changes, the energy destruction rates for working fluid and glass cover are lower than those for absorber plates. Because the output air temperature rises with increasing velocity, Figure 11 demonstrates unequivocally that the exergy destruction rate increases for all solar air heater components. When the velocity rose from 0.9 m/s to 1.7 m/s, the average exergy destruction rate in the absorber plate, working fluid, and glass cover increased by 15.76%, 33.99%, and 38.57%, respectively. As velocity rose from 1.7 m/s to 1.9 m/s, it increased by 18.88%, 19.8%, and 21.65% for the absorber plate, working fluid, and glass cover, respectively.



at v = 1.9 m/s (on 12-May-2019)



at v = 1.7 m/s (on 13-May-2019)



at v = 0.9 m/s (on 14-May-2019)

Figure 11. Hourly variation of exergy destruction rates in the absorber plate, working fluid, and glass cover

The variance in exergy efficiency for different velocities can be seen in Figure 12. The efficiency of the solar air heater increases with increasing velocity, which is due to an increase in the temperature of the outlet air, which increases with increasing velocity. Exergy efficiency increased by 10.34% when the velocity was increased from 0.9 m/s to 1.7 m/s, and it increased by 12.5% when the velocity was increased from 1.7 m/s to 1.9 m/s.

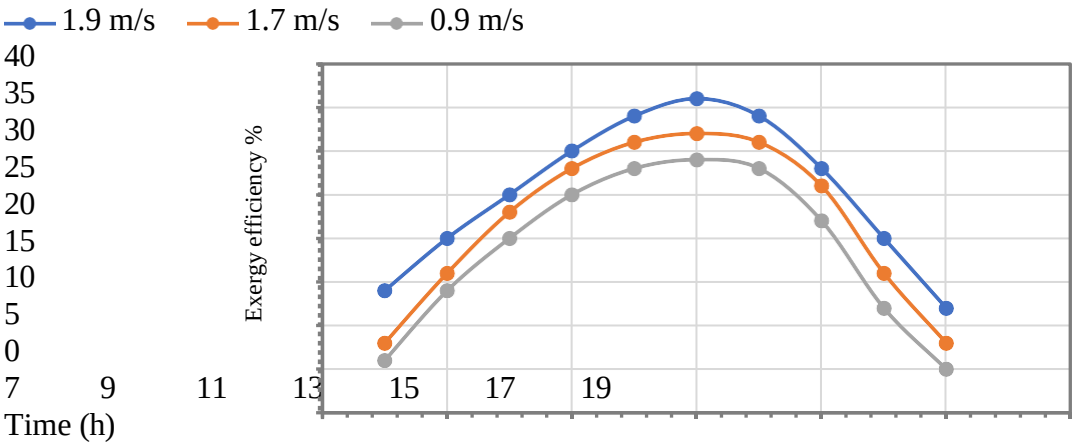


Figure 12. Hourly variation of exergy efficiency at different air velocities

Table 2. Comparison of other studies with the current study

Type of solar air heater	Ref.	Site location	Thermal efficiency (%)
Present study		Iraq	80
Single-pass solar air heater with reflectors and turbulators	[13]	Saudi Arabia	78
Tubular solar heater (TSAH)	[16]	Egypt	84
Solar air heater with (S) shaped ribs with gap	[17]	China	65
Arc-shaped roughened solar air heater	[18]	India	76
Triple-pass solar air heater	[19]	Iraq	80.2
Solar air collectors with different delta turbulators arrangement	[39]	Iraq	88

CONCLUSIONS

The thermal performance of a double-pass solar air heater is examined experimentally in Baghdad, Iraq, using a single line (6 fins) and two lines (12 fins) effect (of L-shaped fins fix) on the top face flat absorber plate. The following is a summary of the work's primary conclusions:

i. The solar air heater's temperature depends on the absorber plate arrangement, flow velocity, and sun intensity.

ii. When the velocity drops from 1.9 m/s to 0.9 m/s, the maximum air exit temperature for the smooth absorber plate rises from 48 °C to 52 °C.

iii. When the velocity shifts from 1.9 m/s to 0.9 m/s, the maximum air exit temperature for the absorber plate with one line of fins rises from 50 °C to 57 °C.

iv. When the velocity changes from 1.9 m/s to 0.9 m/s, the maximum air exit temperature for the absorber plate with two lines of fins rises from 56.5 °C to 64 °C.

v. The fins' greater surface area and the turbulence they create boost efficiency.

vi. For the velocity shift from 0.9 m/s to 1.9 m/s, using a single line of fins increases average efficiency by 21% to 28%.

vii. For the velocity shift from 0.9 m/s to 1.9 m/s, using two lines of fins increases the average efficiency by 50% to 66%.

viii. When the velocity increased from 0.9 m/s to 1.9 m/s, the average exergy destruction rate rose by 37.6%, 60.6%, and 68.66% for absorber plate, working fluid, and glass cover, respectively. iv. The energy efficiency improved by 24.1%.

REFERENCES

In their 2018 article "Potential applications of inserts in solar thermal energy systems - A review to identify the gaps and frontier challenges," Rashidi, Kashefi, and Hormozi discuss the use of inserts in solar thermal energy systems. The study is published in Solar Energy, volume 171, issue 9, and pages 929-952.
The article "Techno-economic study of compound parabolic collector in solar water heating system in the northern hemisphere" was published in the journal Applied Thermal Engineering in 2021 and was written by A. Gilani and S. Hoseinzadeh.
The article "Energy saving in thermal energy systems using dimpled surface technology - A review on mechanisms and applications" was published in 2019 in the journal Applied Energy and was written by S. Rashidi, F. Hormozi, B. Sundén, and O. Mahian.
In 2019, the authors Manikandan, Iniyan, and Goic published a review titled "Enhancing the optical and thermal efficiency of a parabolic trough collector" in the journal Applied Energy. The study was published in volume 235, issue 2, and ran from pages 1524 to 1540.
The following is an excerpt from an article published in 2019 in the Archives of Computational Methods in Engineering: "From topology optimization design to additive manufacturing: today's success and tomorline's roadmap." The authors of the article are L. Meng, W. Zhang, D. Quan, G. Shi, L. Tang, and others.
"A review on heat enhancement in thermal energy conversion and management using Field Synergy Principle," published in Applied Energy in 2020, is authored by X. Zhao, E. Jiaqiang, Z. Zhang, J. Chen, G. Liao, and others.
[7]In "Enhancing thermal conductivity of fluids with nanoparticles," J. Choi and J. Eastman published in 1995 in the ASME International Mechanical Engineering Congress & Exposition (vol. 231, no. October, pp. 99-105).
Nanofluids: synthesis, characteristics and applications, M. Sms and A. Castro, Nova Science Publishers Inc., New York, 2014.
"A critical review of traditional and emerging techniques and fluids for electronics cooling," [9]S. Murshed and D. Castro
Volume 78, Issue 10, October 2017, pages 821–823, Renewable and Sustainable Energy Reviews.
"Investigation of impingement heat transfer for air-sand mixture flow," published in 2016 in The Canadian Journal of Chemical Engineering, was written by M. Al-Dulaimi, A. Rasool, and F. Hamad.
"Experimental investigation on heat transfer augmentation of solar air heater using shot blasted V-corrugated absorber plate," Renewable Energy, vol. 127, no. November, pp.213-229, 2018, by P. Kumar, K. Panchabikesan, L. Deeyoko, and V. Ramalingam.
The article "Experimental study on the performance of spiral solar air heater" was published in Solar Energy in 2019 and was written by B. Jiaa, F. Liu, and D. Wang.
In their 2020 publication "Experimental investigation of single pass solar air heater with reflectors and turbulators," A. Abdullah, M. Amro, M. Younes, Z. Omara, A. Kabeel, and F. Essa reported on their findings. The article can be found in the Alexandria Engineering Journal, volume 59, issue April, pages 579–587.
"Parametric sensitivity analysis and optimization of a solar air heater with multiple lines of longitudinal vortex generators," published in Applied Energy, volume 263, issue April, pages 114556 in 2020, is written by D. Dezan, A. Rocha, and W. Ferreira.
The article "Performance improvement of a solar air heater by covering the absorber plate with a thin porous material" was published in 2020 in the journal Energy and was written by N. Jouybari and T. Lundström.
An experimental examination of the performance of a novel design of solar air heater (tubular)" (Renewable Energy, 2020, vol. 151, no. May, pp. 1055-1066), by H. Hassan, S. Abo-Elfadland M. El-Dosoky.
[17]In "Evaluation of the performance of an improved solar air heater with "S"shaped ribs with gap,"

published in 2020 in Solar Energy, D. Wanga, J. Liu, Y. Liu, Y. Wang, L. Bojia, and J. Liu are the authors.
Thermal performance and heat transfer analysis of arc-shaped roughened solar air heater - An experimental research was published in Solar Energy in 2020 by H. Ghritlahrea, P. Sahu, and S. Chand. The article can be found in volume 199, issue March, pages 173-182.
[19]A study conducted by H. Yassien, O. Alomar, and M. Salih in 2020 examined the effects of incorporating a net of tubes under the absorber surface on the performance of a triple-pass solar air heater system. The findings were published in Solar Energy, volume 207, issue September, pages 813-824.
Applied Thermal Engineering, volume 165, issue 1, pages 113563–133563, 2020, by M. Baissia, A. Brimaa, K. Aouesa, R. Khanniche, and N. Moummi, discusses the thermal behavior in a solar air heater channel that has been roughened by delta-shaped vortex generators.
The paper "Numerical investigation of natural convection solar air heater with different fins shape" was published in 2018 in the journal Renewable Energy and authored by S. Hosseini, A. Ramiar, and A. Ranjbar.
Article published in the International Journal of Thermal Sciences in 2021 by S. Hosseini, A. Ramiar, and A. Ranjbar titled "Thermo-hydraulic performance of a solar air heater with staggered C-shape finned absorber plate" (vol. 168, no. October, pp. 107068).
[23]In their 2019 article titled "Application of nanofluids in thermal performance enhancement of parabolic trough solar collector: state-of-the-art," H. Olia, M. Torabi, M. Bahiraei, M. Ahmadi, M. Goodarzi, and M. Safaei discuss the latest advancements in this field. [24]In their 2019 article titled "Second law of thermodynamics analysis for nanofluid turbulent flow inside a solar heater with the ribbed absorber plate," S. Rashidi, P. Javadi, and J. Esfahani discuss the use of the second law of thermodynamics in solar heaters with ribbed absorber plates.
"Numerical investigation of thermal pulsating alumina/water nanofluid flow over three different cross-sectional channels," submitted by S. Hoseinzadeh, S. Otaghsara, M. Khatir, and P. Heyns in the 2019 edition of the International Journal of Numerical Methods for Heat & Fluid Flow, volume 30, issue 7, pages 3721–3735.
Solar engineering thermal processes, by J. Duffie and W. Beckman, published by John Wiley & Sons in 2013, is a source to consider.
Optimization of solar air collector, P. Matuszewski and M. Sawicka, Aalborg: Aalborg University, 2010.
In their 2002 book "Introduction to Heat Transfer," F. Incropera and D. DeWitt provide a solid foundation in the subject.
In a 2009 article published in the American Journal of Environmental Sciences, the authors [29] Alfegi, Sopian, Othman, and Yatim presented a mathematical model of a fin-equipped double-pass photovoltaic thermal air collector. The model was detailed in volume 5, issue October, pages 592–598.
Thermodynamics in Engineering, Sixth Edition, by M. Moran and H. Shapiro, SI Version [30]. Author: Wiley India (P) Ltd.
Engineering thermodynamics of thermal radiation: for the usage of solar power, by R. Petela, published by McGraw Hill in 2010 (page 31).
Thermodynamics for Advanced Engineers, A. Bejan, Wiley, 2006, Hoboken.
In 1964, R. Petela published an article titled "Exergy of heat radiation" in the ASME Journal of Heat and Mass Transfer, volume 2, issue May, pages 187–192.
"Exergy analysis of the solar cylindrical-parabolic cooker," published in Solar Energy in 2005, volume 79, issue 9, pages 221-233.
A study conducted by M. Karakilcik and I. Dincer in 2008 was published in the International Journal of Thermal Sciences. The study titled "Exergetic performance analysis of a solar pond" included topics such as these.
Experimental examination of energy and exergy performance of square and circular solar ponds, by A. Dehghan, A. Movahedi, and M. Mazidi, published in Solar Energy, volume 97, issue 11, pages 273-284, 2013.

"Exergetic analysis of a solar thermal power system" (Renewable Energy, vol. 19, no. January 2000, pp. 135-143), written by N. Singh, S. Kaushik, and R. Misra.
New York: McGraw Hill Higher Education, 2010. [38]J. Holman, Heat Transfer.
[39]In a 2019 article published in Heat Transfer: Asian Research, Z. Obaid, A. Al-damook, and W. Khalil examine the thermal and economic properties of solar air collectors that use various arrangements of delta turbulators (vol. 48, no. May, pp. 2082-2104).